^1H, ^{47}Ti, and ^{49}Ti ENDOR Study on Frozen Solutions of $[(\eta^5\text{-}C_5H_5)Ti(\eta^8\text{-}C_8H_8)]$ and $[(\eta^5\text{-}CH_3\cdot C_5H_4)Ti(\eta^8\text{-}C_8H_8)]$

Didier Gourier*† and Edmond Samuel‡

Contribution from the Ecole Nationale Superieure de Chimie, 11 rue Pierre et Marie Curie, 75005 Paris, France. *Received October 27, 1986*

Abstract: The paramagnetic mixed sandwich compounds CpTicot and Me–CpTicot (Cp = η^5-C_5H_5, Me–Cp = η^5-CH_3–C_5H_4, cot = η^8-C_8H_8) were studied by ENDOR. It is shown for the first time that signals due to ^{47}Ti and ^{49}Ti nuclei in natural abundance can be resolved in dilute frozen solutions. These data yielded a measure of the quadrupole interaction from which a negative field gradient at the Ti nucleus could be deduced, indicating that the $d_{x^2-y^2}$ and d_{xy} metal orbitals are significantly occupied. Proton ENDOR below 60 K allowed us to measure the principal values of the hyperfine tensor and to deduce proton coordinates from a simple point dipole model. The onset of fast ring reorientation above 60 K is clearly manifested by a gradual transformation of the low-temperature, powderlike ENDOR spectrum into a single crystallike spectrum. The effect of methyl substitution on Cp rings demonstrates that the ring reorientation is only governed by intermolecular interactions.

Studies by ENDOR on paramagnetic complexes, when conducted on dilute single crystals, yield data with a high degree of accuracy and refinement on the magnetic parameters and electronic structure.[1] Such studies have been performed on dibenzene vanadium diluted in paracyclophane[2] and $CoCp_2$ diluted in $MnCp(CO)_3$ matrix.[3] However, dilution in a single crystal host lattice is often problematic, and the more so if the compounds are air and moisture sensitive. In that case, it is preferable to use dilute frozen solutions, but the drawback is loss of resolution resulting from random orientations of the paramagnetic molecules. It was shown, however, that if certain conditions are satisfied, ENDOR offers the possibility to select some molecular orientations.[1,4,5] Our interest in titanium paramagnetic metallocenes incited us to undertake a study of ENDOR on the mononuclear pseudosandwich compounds CpTicot and Me–CpTicot labeled I and II, respectively.

I was synthesized in 1969,[6] and its crystal structure determined.[7,8] Later, attempts were made to determine MO energy levels and schemes were proposed[9,10] whereby from calculations it could be deduced that the positive charge borne by the metal atom was as low as approximately unity. These results were in agreement with XPS studies[11] and were subsequently corroborated by ESR done on frozen solutions[12] which established also the d_{z^2} ground state and provided measurements of the isotropic hyperfine interaction with the ring protons. These data were confirmed by ENDOR studies[13] at 150 K.

However, both ESR and ENDOR conducted at temperatures not lower than 150 K suffer from shortcomings. They do not afford information about (i) the anisotropy of the superhyperfine interaction because of the fast ring rotation at this temperature and (ii) the hyperfine and quadrupole interactions with the ^{47}Ti and ^{49}Ti nuclei.

We show in this work that studies by ENDOR on frozen solutions of I and II between 4 and 130 K, while overcoming the difficulties of matrix dilution mentioned above, allowed us to obtain with precision all the aforementioned magnetic parameters. In particular, we show for the first time that quadrupole interaction with Ti isotopes in natural abundance can be measured on dilute solution samples by this method. Furthermore, we show from studies at variable low temperatures that the aromatic rings undergo fast reorientation around the molecular axis at temperatures above 60 K and that methyl substitution on the Cp ring has a marked influence in raising the temperature threshold for this ring reorientation, without affecting cot reorientation. Also ENDOR gives structural information with a fair degree of precision. The slight discrepancies with X-ray data are discussed.

Experimental Section

All manipulations were conducted under argon. Sample tubes containing the solutions were sealed under vacuum. Solvents were rigorously purified and dried by the conventional methods. Commercial deuteriotoluene was used as received.

I was prepared by literature methods.[6,14] II was prepared by the same procedure as a green crsytalline compound. Both I and II were resublimed under vacuum before use. These two compounds are of low solubility in toluene so that saturated solutions were used to have a satisfactory signal gain. ESR and ENDOR spectra were recorded with a BRUKER ER 220 D X-band spectrometer equipped with an ASPECT-2000 computer-monitored ENDOR unit. Temperatures between 4 and 130 K were obtained with a helium flow cryostat ESR 9 from Oxford Instruments. Typical conditions used for recording the ENDOR spectra were the following: radiofrequency power 100 W; microwave frequency depending on the temperature, 4 mW for protons at 30 K; 13 mW for titanium at 30 K; 100 mW for protons at 100 K. A 12.5-kHz frequency modulation of the rf field was used with a deviation of ±50 kHz for protons and ±150 kHz for titanium. Single sweeps of 200 s were sufficient to obtain very good signal-to-noise ratio.

Results

Figure 1 shows the ESR spectrum of I in glassy toluene at 30 K. It is easily interpreted in terms of an unpaired spin $S = {}^1/_2$ of a Ti^3 ($3d^1$) ion having axial symmetry. The most important portion of the spectrum is due to molecules containing titanium with nonmagnetic nuclei ($I = 0$). The electron g spectra $g_\parallel$ = 2.000 (8) and $g_\perp$ = 1.972 (3) show that the unpaired electron is confined in the nonbonding $a_1(3dz^2)$ orbital.[13] Weak satellites detectable in the high and low field sides of the spectrum result from the hyperfine (hf) interaction of the electron spin with the ^{47}Ti ($I = {}^5/_2$, $g_n = -0.31484$, abundance 7.75%) and ^{49}Ti ($I = {}^7/_2$, $g_n = -0.31491$, abundance 5.51%) nuclei. The hf parameters $A_\perp$ = 56 MHz and $A_\parallel \sim 10$ MHz could not be obtained with accuracy principally due to poor resolution and also because the ESR spectrum of molecules containing ^{47}Ti and ^{49}Ti nuclei is almost completely obscured by the intense spectrum of titanium with zero nuclear spin. Moreover it is impossible to separate hf transitions of ^{47}Ti and ^{49}Ti since their nuclear g factors are almost

†Laboratoire de Chimie de la Matiere Condensee (UA 302 CNRS).
‡Laboratoire de Chimie Organique Industrielle (UA 403 CNRS).

(1) Schweiger, A. *Struct. Bonding (Berlin)* **1982**, 51.
(2) Wolf, R.; Schweiger, A.; Gunthard, H. *Mol. Phys.* **1984**, *53*, 567; **1984**, *53*, 585.
(3) Rudin, M.; Fauth, J. M.; Schweiger, A.; Ernst, R. R.; Zoller, L.; Ammeter, J. H. *Mol. Phys.* **1983**, *49*, 1257.
(4) Rist, G. H.; Hyde, J. S. *J. Chem. Phys.* **1970**, *52*, 4633.
(5) Hoffman, B. M.; Martinsen, J.; Venters, R. A. *J. Magn. Reson.* **1984**, *59*, 110.
(6) Van Oven, H. O.; de Liefde Meijer, H. J. *J. Organomet. Chem.* **1969**, *19*, 373.
(7) Zeinstra, J. D.; de Boer, J. L. *J. Organomet. Chem.* **1973**, *54*, 207.
(8) Kroon, P. A.; Helmholdt, R. B. *J. Organomet. Chem.* **1970**, *25*, 451.
(9) Clack, D. W.; Warren, K. D. *Inorg. Chim. Acta* **1977**, *24*, 35.
(10) Clack, D. W.; Warren, K. D. *Theor. Chim. Acta* **1977**, *46*, 313.
(11) Evans, S.; Green, J. C.; Jackson, S. E. *J. Chem. Soc., Dalton Trans.* **1974**, 304.
(12) Samuel, E.; Labauze, G.; Vivien, D. *J. Chem. Soc., Dalton Trans.* **1979**, 956.
(13) Labauze, G.; Raynor, J. B.; Samuel, E. *J. Chem. Soc., Dalton Trans.* **1980**, 2425.
(14) Kool, L. B.; Rausch, M. D.; Rogers, R. D. *J. Organomet. Chem.* **1985**, *297*, 289.

0002-7863/87/1509-4571$01.50/0

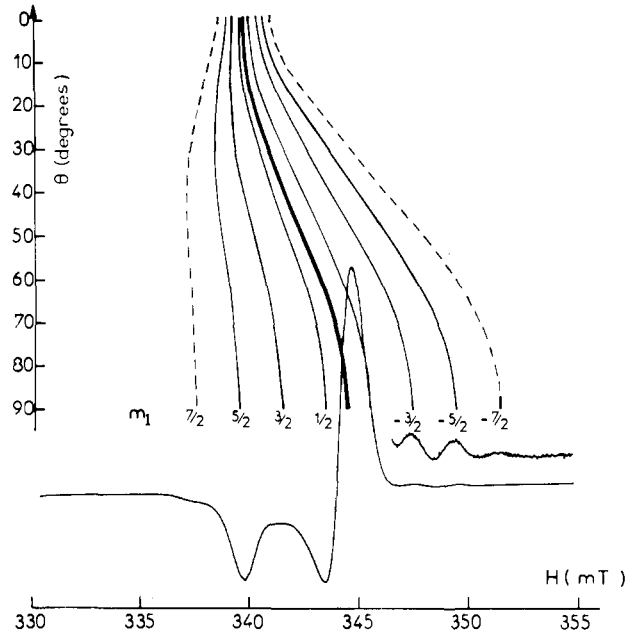

Figure 1. ESR spectrum at 30 K of CpTicot diluted in toluene and theoretical variation of the line position with the angle θ between the molecular axis and the magnetic field $\vec{H}$.

identical. Figure 1 also shows the theoretical angular variation of the ESR spectrum. This diagram will be useful to interpret the selection of molecular orientations performed in the ENDOR experiments.

In the following discussion, we assume that g and titanium hf tensors are perfectly axial with their c_∞ axes parallel to the ring-titanium-ring axis. This is a reasonable assumption since the two rings are parallel, which implies that the complex has a nearly axial symmetry although its exact symmetry is not higher than C_s.

The ENDOR spectra were obtained by partially saturating the ESR spectrum at a given magnetic field value while sweeping the radiofrequency (rf) field. At 30 K, the ENDOR spectrum is composed of two different parts: an intense spectrum with eight transitions centered around the proton frequency; its intensity strongly decreases when the magnetic field is set on the hf satellites. The other part of the ENDOR spectrum is composed of several transitions in the region 22–32 MHz, and its intensity is approximately constant in all the magnetic field range which spans the total ESR spectrum. These two different spectra correspond to proton ENDOR and to ENDOR of ^{47}Ti and ^{49}Ti, respectively.

(1) ENDOR of ^{47}Ti and ^{49}Ti. The principal characteristics of this powder ENDOR spectrum is that both the number of transitions and their positions strongly depend on the magnetic field setting, as shown on Figure 2. Despite this variation, all these transitions are due to molecules with the same orientation with respect to the magnetic field direction as will be shown below. Since the hf parameters $A(\theta)$ lie between 10 and 56 MHz (θ being the angle between the direction of the magnetic field and the symmetry axis of the molecule), $A/2$ is always larger than the nuclear frequency ν_n = 0.84 MHz (at 350 mT). Consequently the ENDOR frequencies satisfy the condition

$$\nu = |A(\theta)/2 \pm \nu_n| \quad (1)$$

if we neglect the quadrupole interactions for the moment. All the detectable transitions are at frequencies between 22 and 32 MHz, which implies that $A(\theta)$ is in the range 45–60 MHz and thus corresponds to θ values roughly in the region 60–90°.

It should be pointed out that except for angles around θ = 0° and θ = 90° the hf interaction varies rapidly with θ so that ENDOR signals should be difficult to observe. Furthermore, $A_\parallel/2$ being of the order of 5–10 MHz, the ENDOR transitions corresponding to θ = 0 should be hidden in the strong proton ENDOR spectrum. Consequently all the detectable part of the titanium ENDOR spectrum should contain transitions at $A_\perp/2 \pm \nu_n$. This is evident if the magnetic field is set at the $m_I = -^7/_2$ ESR transition (Figure 1). In that case only molecules with $\theta = \pi/2$ and containing ^{49}Ti nuclei are selected. Furthermore, if the magnetic field is set at the $m_I = ^1/_2$ ESR transition, for example, both ^{49}Ti and ^{47}Ti contribute to the ENDOR spectrum, and many angles θ are selected. However, only transitions corresponding to $\theta = \pi/2$ vary slowly with θ, so that the transitions corresponding to the other selected angles θ are not detectable. For these reasons, all the observed titanium ENDOR transitions were accurately interpreted as transitions of molecules with their axis perpendicular to the magnetic field.

Figure 2 shows the eight ENDOR spectra obtained with the field settings $m_I = \pm^7/_2, \pm^5/_2, \pm^3/_2$, and $\pm^1/_2$. They were interpreted by using the spin Hamiltonian for axial symmetry[15]

$$\mathcal{H} = \beta H(g_\parallel S_z \cos\theta + g_\perp S_x \sin\theta) + A_\parallel S_z I_z + A_\perp(S_x I_x + S_y I_y) - g_n\beta_n H I_z + P_\parallel\{I_z^2 - \tfrac{1}{3}I(I+1)\} \quad (2)$$

where the different terms represent the electronic Zeeman, the hyperfine, the nuclear Zeeman, and the quadrupole interactions, respectively. The z axes of the g, hf, and quadrupole tensors have been taken parallel to the molecular axis. Since titanium has two isotopes, two spin Hamiltonians of this type are necessary to interpret the spectra. The solutions, up to the second order in perturbation for $\theta = \pi/2$, give the energy of the spin states when H is perpendicular to the molecular axis

$$E(m_s, m_I) = g_\perp\beta H_o m_s - g_n\beta_n H_o m_I + A_\perp m_s m_I + \frac{A_\parallel^2 + A_\perp^2}{4g_\perp\beta H_o} m_s[I(I+1) - m_I^2] - \frac{1}{2}P_\parallel\left[m_I^2 - \frac{1}{3}I(I+1)\right] + \frac{P_\parallel^2}{8A_\perp m_s} m_I\{2I(I+1) - 2m_I^2 - 1\} \quad (3)$$

We have omitted small terms which have a negligible contribution to the spectrum. The $m_s = \pm^1/_2$ portion of the energy level diagram is shown on Figure 3 for $A_\perp > 0$ and g_n, $P_\parallel < 0$. For the moment we assume that there is no significant relaxation between different m_I states within a given m_s state (i.e., long nuclear spin lattice relaxation time T_{1n}) and that only the simple type of cross relaxation process $(m_s, m_I) \leftrightarrow (m_s - 1, m_I \pm 1)$ contributes to the ENDOR response. Under these conditions, if the magnetic field is set at the ESR transition m_I, only the NMR transitions $(m_I \leftrightarrow m_I \pm 1)+$ and $(m_I \leftrightarrow m_I \pm 1)-$ desaturate the ESR transition. (The signs + and − represent the m_s states $m_s = +^1/_2$ and $m_s = -^1/_2$.) We thus expect two ENDOR transitions for each m_s state and for each Ti isotope, except when $m_I = \pm I$, for which only one ENDOR line is expected. An example is shown on Figure 3, where the ESR transition $m_I = +^5/_2$ is saturated. We have calculated the position of ENDOR lines by using expression 3. The relative intensity of the transitions was obtained by taking into account only the natural abundance of ^{47}Ti and ^{49}Ti and a hf enhancement factor $(\nu/\nu_n)^2$. The best fit with the experimental spectra was found by using the following parameters $A_\perp(^{47}\text{Ti}) = +52.8 \pm 0.05$ MHz, $P_\parallel(^{47}\text{Ti}) = -2.3 \pm 0.02$ MHz, $A_\perp(^{49}\text{Ti}) = +52.4 \pm 0.05$ MHz, and $P_\parallel(^{49}\text{Ti}) = -0.9 \pm 0.02$ MHz, Table I. The sign of $A_\perp$ was determined by ESR,[13] and the results clearly show that $P_\parallel$ and g_n have the same sign, thus $P_\parallel$ is negative.

It should be noticed that there are some discrepancies concerning the intensities of the calculated and experimental transitions. Examination of Figure 2 indicates that several transitions are much weaker than expected, and several unexpected weak transitions occur, particularly at high frequency. This is most probably related to the simplicity of the assumptions concerning the relaxation paths. Weak additional transitions can occur if the relaxation between different m_I states within a given m_s state is not negligible. Such transitions are visible on the spectra obtained with field settings $m_I = \pm^1/_2$. The case of the weak ENDOR transitions at high frequency, observed with the field settings $m_I = \pm^7/_2$, appears differently. When the ESR transitions $m_I = \pm^7/_2$ are saturated we observe only molecules containing a ^{49}Ti nucleus (see Figure 1), and we thus expect only ENDOR transitions $(+^7/_2 \leftrightarrow +^5/_2)\pm$ and $(-^5/_2 \leftrightarrow -^7/_2)\pm$ of ^{49}Ti. However,

(15) Abragam, A.; Bleaney, B. *Electron Paramagnetic Resonance of Transition Metal ions*; Clarendon Press: Oxford, 1971.

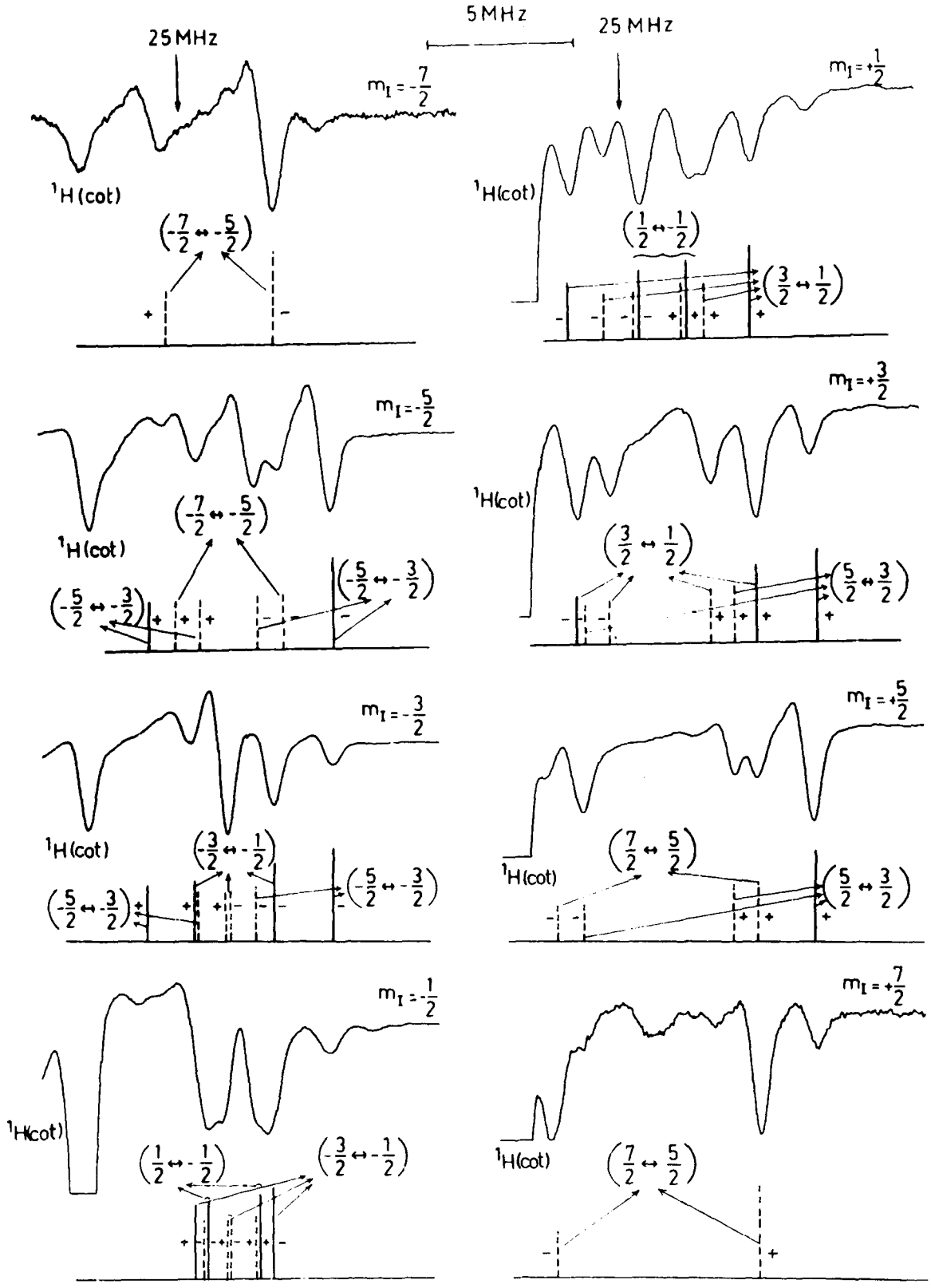

Figure 2. ENDOR spectra at 30 K of ^{47}Ti and ^{49}Ti in CpTicot diluted in deuteriotoluene. The magnetic field is set at the maximum of the eight hyperfine lines of the ESR spectrum. Each ENDOR spectrum is labeled by the m_I value of the ESR transition observed. The transition at low frequency in each spectrum is a proton ENDOR transition of the cot rings. The stick diagrams show the calculated ENDOR transitions. The signs + and − represent the m_s states. The m_I states connected by the ENDOR transitions are shown in parentheses. ^{47}Ti and ^{49}Ti transitions are represented by full and dashed lines, respectively.

these fields settings also produce ENDOR transitions ($+^5/_2 \leftrightarrow +^3/_2$)+ and ($-^3/_2 \leftrightarrow -^5/_2$)− of ^{47}Ti. We have verified that this is true even when we saturate the high field flank of the ESR transition $m_I = -^7/_2$, where hf pattern of ^{47}Ti has no contribution. Since ^{47}Ti and ^{49}Ti do not belong to the same molecule, these extra ENDOR transitions point to the existence of some relaxation paths between m_I states belonging to different molecules, some containing a ^{49}Ti nucleus and others a ^{47}Ti nucleus. If such a relaxation mechanism exists, the intensity of the extra lines should be a function of concentration. However, it was not possible to confirm this experimentally because a decrease of the concentration produced a collapse of all ENDOR transitions and because ENDOR experiments were conducted anyway with saturated solutions.

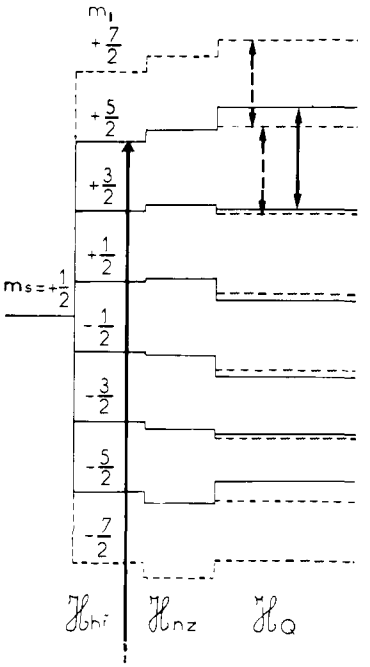

Figure 3. $m_s = +^1/_2$ portions of the energy level diagrams of a $S = {}^1/_2$ electron spin interacting with ^{47}Ti and ^{49}Ti nuclei. The diagrams for the two nuclei are superimposed, although they belong to different molecules. H_{HF}, H_{ZN}, and H_Q represent the hyperfine, nuclear Zeeman, and quadrupole interactions, respectively. These different interactions are not to scale: $A_\perp > 0$, $g_n < 0$, $P_\parallel < 0$, and $^{47}P_\parallel/^{49}P_\parallel = 2.6$. Also shown are the ENDOR transitions obtained by saturating the ESR transition $m_I = +^5/_2$. The energy levels and ENDOR transitions of ^{47}Ti and ^{49}Ti are represented by full lines and dashed lines, respectively.

Table I. ^{47}Ti and ^{49}Ti ENDOR Parameters of CpTicot in Deuteriotoluene

	$A_\perp$ (MHz)	$P_\parallel$ (MHz)
^{47}Ti	+52.8 ± 0.005	−2.3 ± 0.02
^{49}Ti	+52.4 ± 0.005	−0.9 ± 0.02

ENDOR Induced Electron Spin Resonance (E.I.E.). In this type of experiment, one observes the intensity of a given ENDOR line as a function of the magnetic field.[16,17] With the modulation scheme employed, the result is displayed as an absorption ESR spectrum instead of a first derivative as in conventional ESR spectroscopy. Furthermore the spectrum obtained is only that part of the ESR spectrum which is due to molecules containing ^{47}Ti or ^{49}Ti. As a consequence we obtain an ESR spectrum with a hyperfine pattern which is undetectable in a conventional ESR spectrum because it is hidden in the intense spectrum of molecules containing titanium with zero nuclear spins. We used these EIE spectra to find the positions of the different hf transitions and thus the different magnetic field settings for the ENDOR spectra of Figure 2. It must be pointed out that the ENDOR transitions observed belong to CpTicot with their molecular axis making an angle of $\pi/2$ with the magnetic field. Consequently, the EIE obtained are single crystallike ESR spectra. If the simple assumptions made above concerning the relaxation paths are valid, only the two ESR transitions which belong to the m_I values connected by the observed ENDOR transition are obtained. For example, the two ESR transitions $m_I = +^5/_2$ and $m_I = +^3/_2$ are displayed when the radiofrequency field is set at the transition $(^5/_2 \leftrightarrow {}^3/_2)+$ of ^{47}Ti. The resulting EIE spectrum is shown in Figure 4a. It should be emphasized that this spectrum is only due to molecules containing ^{47}Ti nuclei, although the ESR transitions of ^{47}Ti and ^{49}Ti are completely superimposed in conventional ESR. On the other hand, if the radiofrequency field is set at a position where several ENDOR transitions occur, the EIE spectrum is composed of several pairs of ESR transitions. An example

(16) Anderson, W. A. *J. Chem. Phys.* **1962**, *27*, 1373. Hyde, J. S. *J. Chem. Phys.* **1965**, *43*, 1806.
(17) Niklas, J. R.; Spaeth, J. M. *Phys. State Solid (B)* **1980**, *101*, 221.

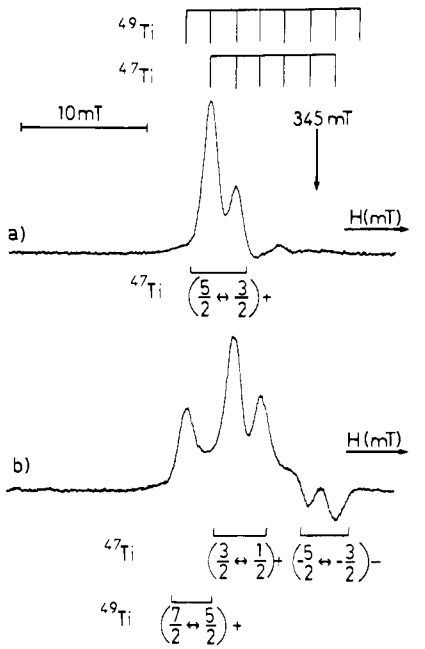

Figure 4. ENDOR-induced ESR spectra (EIE) of CpTicot diluted in deuteriotoluene, T = 30 K: (a) radiofrequency field setting ν = 31.3 MHz and (b) radiofrequency field setting ν = 29.5 MHz.

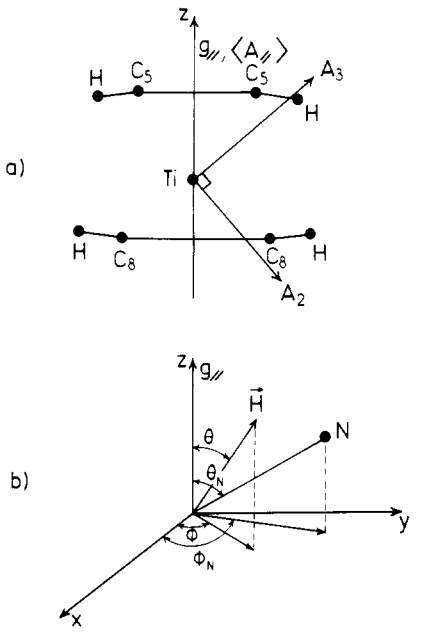

Figure 5. (a) Principal axes system of the proton hyperfine interaction and (b) coordinate system used for ENDOR experiment.

is shown in Figure 4b. This rf field setting corresponds to the ENDOR transitions $(^7/_2 \leftrightarrow {}^5/_2)+$ of ^{49}Ti, $(^3/_2 \leftrightarrow {}^1/_2)+$ of ^{47}Ti, and also to the flank of the ENDOR transition $(-^5/_2 \leftrightarrow -^3/_2)\pm$ of ^{47}Ti nuclei. This is the reason by the two EIE transitions $m_I = -^3/_2$ and $m_I = -^5/_2$ appear as weak negative signals. We have failed to observe ENDOR transitions centered around $A_\parallel$ because they are completely hidden in the intense proton ENDOR spectrum.

(2) Proton ENDOR. (a) ENDOR Line Shape in Frozen Solution. (In section 2, A will refer to the proton hyperfine interaction.) To clarify the interpretation of the experimental results, we shall first consider the effect of ring dynamics on the ENDOR line shape. For molecules of I containing only titanium nuclei with zero nuclear spins, the ESR spectrum is composed of only one transition with position determined only by the anisotropy of g since the proton interaction is not resolved. The spectrum of Figure 1 reflects the powder average of all complex orientations with respect to the static magnetic field. The z axis of the g tensor

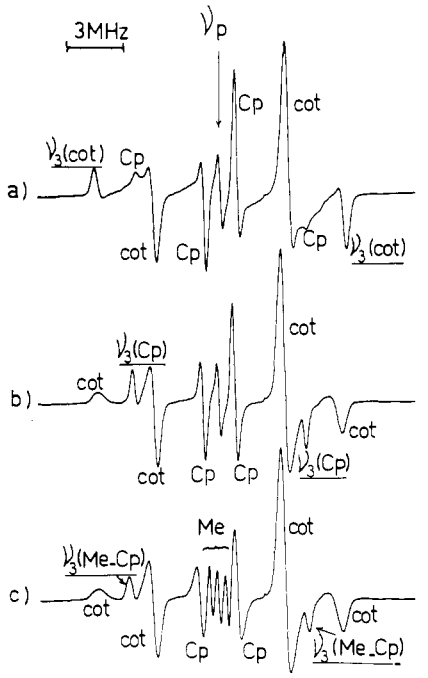

Figure 6. Proton ENDOR in deuteriotoluene at 30 K of (a) CpTicot with $\tilde{H}$ parallel to the A_3(cot) axis, (b) CpTicot with $\tilde{H}$ parallel to the A_3(Cp) axis, and (c) MeCpTicot with $\tilde{H}$ parallel to the A_3(Cp) axis.

being parallel to the molecular axis, if we partially saturate a part of the ESR spectrum corresponding to a resonant field value H_o, we select molecules with symmetry axis making an angle θ with $\tilde{H}$ (Figure 5) given by

$$\theta = \cos^{-1}\left\{\left[\left(\frac{h\nu}{\beta H_o}\right)^2 - g_\perp{}^2\right]/[g_\parallel{}^2 - g_\perp{}^2]\right\}^{1/2} \quad (4)$$

If now a fixed proton with coordinates R_N, θ_N, and ϕ_N interacts with the electron spin, with hf parameters A_i (i = 1, 2, 3), and with the A_3 axis approximately along the Ti–H direction and $A_2 = A_1$, we expect an ENDOR spectrum composed of two peaks at frequencies[15,18]

$$\nu(m_s) = \left[\sum_{i=1}^{3}\left(\frac{m_s}{g}g_i h_i A_i - h_i \nu_p\right)^2\right]^{1/2} \quad (5)$$

where h_i is the direction cosine between the magnetic field and the ith hyperfine tensor axis and

$$g^2 = \sum_{i=1}^{3} h_i{}^2 g_i{}^2 \quad (6)$$

However, even if a single molecule orientation θ is selected by the field setting, the angle ϕ can assume all the possible values between 0 and 360°. For this reason the ENDOR spectrum will be a powder average of all the possible values of the angle ϕ and will present a characteristic powder line shape, with two peaks for each m_s state due to a slower variation of $\nu(m_s)$ with ϕ.[4,5,18] Since the protons of each ring are identical, they will give the same spectrum. Consequently the ENDOR will consist of eight peaks, two for each ring and for each m_s state. It is however possible to obtain the hf parameters A_i by varying the field setting H_o and thus the selected angle θ. This is valid at low temperatures (e.g., ~ 4 K) at which the rings are assumed to be immobilized. If the temperature is raised, the rings can undergo uniaxial reorientation around the molecule axis.[2] However, if the ring reorientation is slow compared to the time scale of the ENDOR experiment (of the order of the anisotropy of the hf coupling), the line shape will remain of powder type.

If, on the other hand, the rings undergo fast reorientation compared to ENDOR time scale, the hf interaction will be partially averaged, with new values $\langle A_\parallel \rangle$ and $\langle A_\perp \rangle$. The z axis of the hf tensor is now parallel to the molecular axis and thus to the z axis of the g tensor. The important difference with the preceding case (slow reorientation) lies in the line shape. Expression 5 giving the ENDOR frequencies is now reduced to

$$\nu(m_s) = \left[\left(\frac{m_s}{g}g_\parallel\langle A_\parallel\rangle - \nu_p\right)^2 \cos^2\theta + \left(\frac{m_s}{g}g_\perp\langle A_\perp\rangle - \nu_p\right)^2 \sin^2\theta\right]^{1/2} \quad (7)$$

At each selected angle θ, we expect only two ENDOR frequencies for each ring, and the spectrum is now single crystallike.

In conclusion there are two types of line shapes depending on the frequency of ring reorientation: for slow reorientation the line shape is powderlike. In the case of fast reorientation the line shape is single crystallike at any field setting. These features can be related to the angle between the z axes of the g and hf tensors. The powder line shape is related to a finite angle θ_N between the two axes. The onset of fast ring reorientation is equivalent to a rotation of $-\theta_N$ of the hf tensor axis, making the two axes coincident and leading to a single crystallike line shape.

Table II. Proton ENDOR Parameters of CpTiCot in Deuteriotoluene

A (MHz)	Cot	Cp
A_3	+13.4 (0)	+9.3 (0)
A_2	+6.2 (2)	+1.4 (0)
A_1	+6.7 (2)	+1.5 (0)
A_{iso}[a]	+8.7 (8)	+4.0 (7)
A_3^{dip}	+4.6 (2)	+5.2 (3)
A_2^{dip}	−2.5 (6)	−2.6 (7)
A_1^{dip}	−2.0 (6)	−2.5 (7)
$\langle A_\parallel \rangle$	+7.41	+4.91
$\langle A_\perp \rangle$	+9.46	+3.68
A_{iso}[b]	+8.78	+4.09

[a] Obtained from A_i. [b] Obtained from $\langle A_\parallel \rangle$ and $\langle A_\perp \rangle$.

Table III. Proton ENDOR Parameters of MeCpTiCot in Deuteriotoluene[a]

A (MHz)	Me–Cp	A (MHz)	Me–Cp
A_3	+9.4 (9)	A_2^{dip}	−2.6 (3)
A_2	+1.6 (5)	A_1^{dip}	−2.5 (7)
A_1	+1.7 (1)	$\lvert A_{max}^{CH_3}\rvert$	0.9
A_{iso}	+4.2 (8)	$\lvert A_{min}^{CH_3}\rvert$	0.7
A_3^{dip}	+5.2 (1)		

[a] Parameters for Cot protons are exactly the same as in CpTiCot.

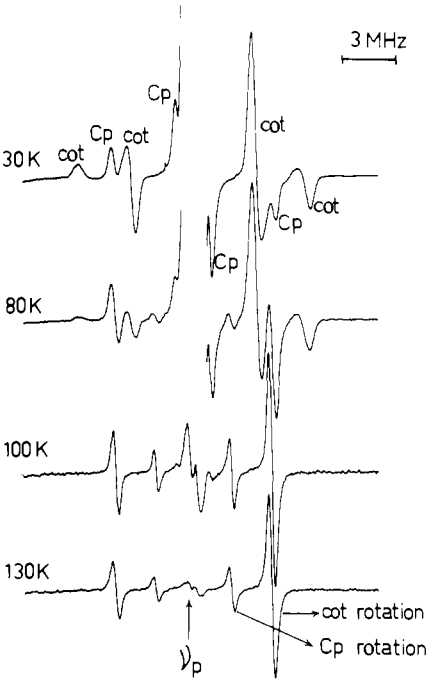

Figure 7. Temperature dependence of the ENDOR spectrum of CpTicot in toluene.

(18) Hurst, G. L.; Henderson, T. A.; Kreilick, R. W. *J. Am. Chem. Soc.* **1985**, *107*, 7294.

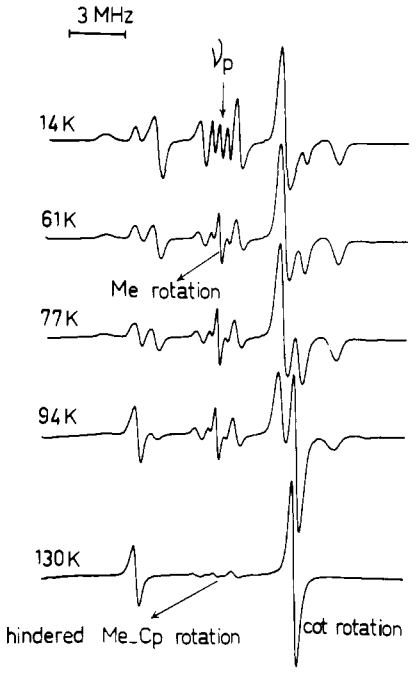

Figure 8. Temperature dependence of the ENDOR spectrum of MeCpTicot in deuteriotoluene.

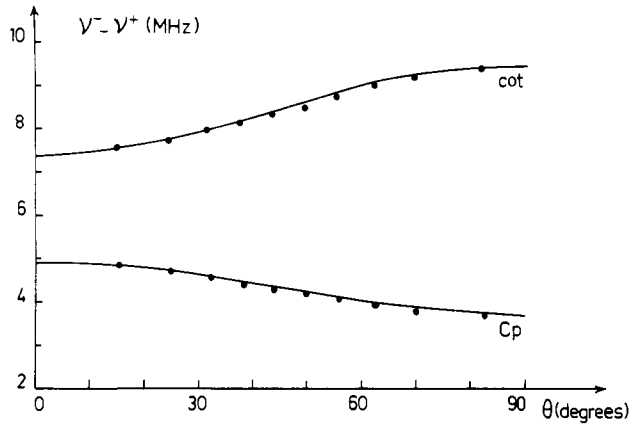

Figure 9. Proton ENDOR of CpTicot at 100 K. Variation of $\nu^- - \nu^+$ with the selected angle θ: points, experimental values; full line, calculated.

(b) Proton ENDOR in the Temperature Range 4–130 K. Proton ENDOR spectra at 30 K of I diluted in frozen deuteriotoluene are shown in Figure 6. They exhibit a powder line shape with eight peaks almost symmetrically disposed around the proton frequency ν_p. The line shape is identical at 4 K. The general features of the spectra do not change upon variation of the field setting except for the frequencies and widths of the two sets of the outermost transitions. The frequencies of the four other transitions vary only slowly with the field setting. In order to identify the protons and to obtain the principal values A_3 of the hf tensors, the magnetic field has been swept stepwise across the ESR spectrum. When the field setting is such that the selected angle θ is equal to θ_N for one proton, two ENDOR transitions reach their maximum frequency shift from ν_p, and their line width is minimum. For these special cases, illustrated in Figure 6 (parts a and b), the field direction cosine h_3 is unity and expression 5 for the ENDOR frequencies is reduced to

$$\nu_3(m_s) = \nu_p \pm A_3/2 \qquad (8)$$

The assignment of the ENDOR transitions to Cp and cot rings was made by noticing that the two field settings which gave the maximum ENDOR shifts correspond, through expression 3, to angles $\theta \simeq 65° \pm 3°$ and $\theta = 45° \pm 3°$. These values are close to $\theta_N = 64°$ and $\theta_N = 48.2°$ obtained for cot and Cp protons by using x-ray diffraction data. With expression 8 we obtained A_3(cot) = 13.4 (0) MHz and A_3(Cp) = 9.3 (0) MHz. Taking into account the isotropic hf coupling values A_{iso} measured by ESR in liquid solution,[13] a complete identification of the other ENDOR transitions was thus made possible, as shown in Figure 6. The results also show that the hf tensor is nearly axial for Cp rings and orthorhombic for cot rings. The cot protons exhibit the smallest ENDOR shifts with a field setting corresponding to $\theta \simeq 22 \pm 5°$. We thus obtain A_2(cot) = 6.2 (2) MHz. It should be pointed out that the selected angle is close to $\pi/2 - \theta_N$. The A_2 axis is thus in the plane containing the molecular axis and the A_3 axis, and the A_1 axis is approximately parallel to the ring plane (see Figure 5a). The hf parameters A_1(cot) = 6.7 (2) MHz was measured by setting the magnetic field at the high field flank of the ESR spectrum, corresponding to $\theta = \pi/2$. Similar measurements for Cp protons gave A_2(Cp) = 1.4 (0) MHz and A_1(Cp) = 1.5 (0) MHz.

The protons hf tensor can be decomposed into the isotropic part A_{iso} and the dipolar part A_i^{dip}

$$A_{iso} = (\sum_{i=1}^{3} A_i)/3$$

$$A_i^{dip} = A_i - A_{iso} \qquad (9)$$

All the proton hf parameters A_i, A_i^{dip}, and A_{iso} are gathered in Table II. For the determination of the relative signs of the hf components, we have considered that A_3 being larger than A_2 and A_1, the isotropic part A_{iso}, and the component A_3^{dip} of the dipolar coupling must have the same sign. Since A_3^{dip} is positive, A_{iso} is also positive, and it follows that A_3 is positive. Furthermore approximate values of A_{iso} for Cp and cot were measured by ESR.[12] Using these values, the only possibility is that A_1, A_2, and A_3 are all positive. Exactly the same ENDOR spectra and hf parameters were obtained for I diluted in frozen Me–THF. Proton ENDOR spectra of II in deuteriotoluene exhibit very similar features as shown in Figure 6c. In particular the hf parameters for cot protons are identical within experimental errors to those of CpTicot. For protons of Me–Cp rings however the parameters are slightly different from those of Cp rings as shown in Table III. Additional lines around the proton frequency are due to methyl protons, with two coupling values $|A_{max}| = 0.9$ MHz and $|A_{min}| = 0.7$ MHz depending on the field setting. These obser-

Table IV. Titanium Proton Distances R_N and Angle θ_N between the Molecular Axis and the A_3 Axis[a]

	cot rings		Cp rings	
	R_N (Å)	θ_N	R_N (Å)	θ_N
ENDOR	3.25	66°	3.11	48.5°
X-rays	3.19	64°	3.00	48.2°

[a] R_N is obtained from the point dipole–dipole expression 16.

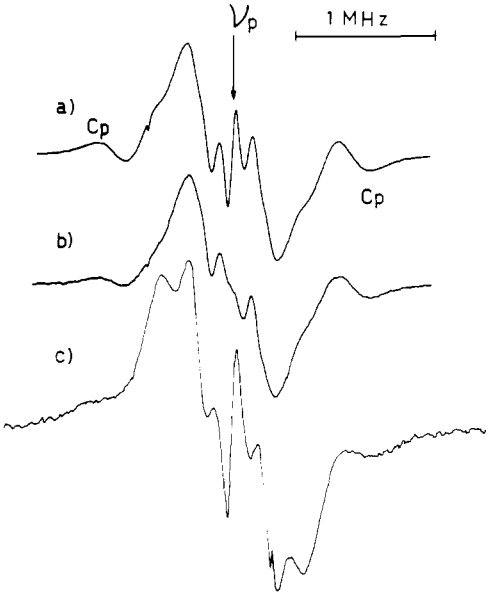

Figure 10. Proton matrix ENDOR of CpTicot in (a) toluene at 30 K, (b) toluene at 80 K, and (c) MeTHF at 30 K.

vations establish without ambiguity the identity of the compound.

The temperature dependances of the proton ENDOR spectra of I in toluene and of II in deuteriotoluene are shown in Figures 7 and 8. The presence of a strong matrix signal for I is due to the protons of toluene molecules, and the evolution of this matrix ENDOR with temperatures will be considered later. Despite the similarity of the ENDOR spectra of I and II at low temperature, their respective evolution with temperature is different, and we shall consider first CpTicot. Upon increasing T from 30 to 100 K, a single crystallike spectrum superimposed on the powderlike spectrum appears. The new signal is detectable at about 60 K, and its intensity increases with T while the powderlike spectrum progressively decreases and vanishes around 90–95 K. The single crystal character of the new spectrum is clearly shown in Figure 9, which represents the evolution of $(\nu^- - \nu^+)$, the difference between the ENDOR frequencies, with the selected angle θ calculated with use of expression 4. The experimental points are fitted with curves calculated with use of expression 7 and the $\langle A_\parallel \rangle$ and $\langle A_\perp \rangle$ values for Cp and cot given in Table II. The plot of Figure 9 is tantamount to a rotation of a single crystal in the magnetic field. The single crystal character of the spectra is related to the coincidence of the z axes of the g and hf parameters and is thus produced by the fast reorientation of cot and Cp rings around the molecular axis.

The two components $\langle A_\parallel \rangle$ and $\langle A_\perp \rangle$ of the partially averaged hf tensor can be related to the hf tensor of static rings by

$$\langle A_\parallel \rangle = A_2 \sin^2 \theta_N + A_3 \cos^2 \theta_N$$

$$\langle A_\perp \rangle = \tfrac{1}{2}(A_2 \cos^2 \theta_N + A_1 + A_3 \sin^2 \theta_N) \qquad (10)$$

$$A_{iso} = \tfrac{1}{3}(\langle A_\parallel \rangle + 2\langle A_\perp \rangle)$$

The values $A_{iso}(cot) = +8.78$ MHz and $A_{iso}(Cp) = +4.09$ MHz calculated with use of expression 10 are in complete agreement with those measured at low temperature (see Table II) but are more precise because of the single crystal character of the spectra. This good agreement proves the validity of the hf parameters measured at low temperature. Expression 10 can be used to get more precise values of the angles θ_N than with use of expression 4. With the experimental values of A_i, $\langle A_\parallel \rangle$, and $\langle A_\perp \rangle$, we found $\theta_N = 66°$ and $\theta_N = 48.5°$ for cot and Cp protons, respectively. There is a good agreement with the values $\theta_N = 64°$ and $\theta_N = 48.2°$ (Table IV) obtained from X-ray data.[8]

The behavior of II upon increasing T is significantly different, as shown in Figure 8. Between 30 and 60 K appears a modification of the spectrum near ν_p due to the onset of methyl rotation around a C–C axis. At about 60 K also appears the single crystallike ENDOR of fastly reorienting cot rings. This signal also increases with T while the powderlike spectrum progressively disappears. However, no signal attributable to rotating Cp rings are detectable at high temperature, but at 130 K the "perpendicular" transitions of static Cp rings are still detectable. This implies that these rings do not exhibit reorientation or, rather, that the frequency of reorientation is slow compared to ENDOR time scale, which is of the order of $^1/_2(A_3 - A_1) \simeq 4$ MHz. The methyl group thus strongly hinders the Cp rotation but does not perturb the cot rotation.

(c) Matrix ENDOR. The proton matrix ENDOR signal is due to purely dipolar interaction between the electron spin and the protons of the solvent cage containing the complex. Such signals are shown in Figure 10 for I in toluene and Me–THF. In both cases the signal is partially resolved, but the resolution is better for Me–THF. The matrix ENDOR line shape is completely independent of the field setting, which indicates that the protons of the solvent cage are randomly distributed around the paramagnetic complex. The two broad features flanking the matrix signal are due to dipolar interaction with the nearest proton neighbors of the cage. Thus the corresponding ENDOR frequencies are given by

$$\nu = \nu_p \pm g\beta g_N \beta_N R^{-3} \qquad (11)$$

where R is titanium–proton cage distance. For both toluene and Me–THF solvent we found $R = 5.4$ Å. The cage radius thus seems to be imposed by the complex rather than the solvent. The temperature dependence of the matrix line shape is shown in Figures 10 and 7 for toluene. At about 80 K the ENDOR transitions of nearest cage protons begin to decrease, indicating the onset of a motion of cage molecules. It is worth noticing that this temperature is also that at which fast ring reorientation in I appears. Between 80 and 130 K, the intensity of the matrix signal strongly decreases due to a complete averaging of the electron–proton cage dipolar interaction (see Figure 7) by the motion of toluene molecules.

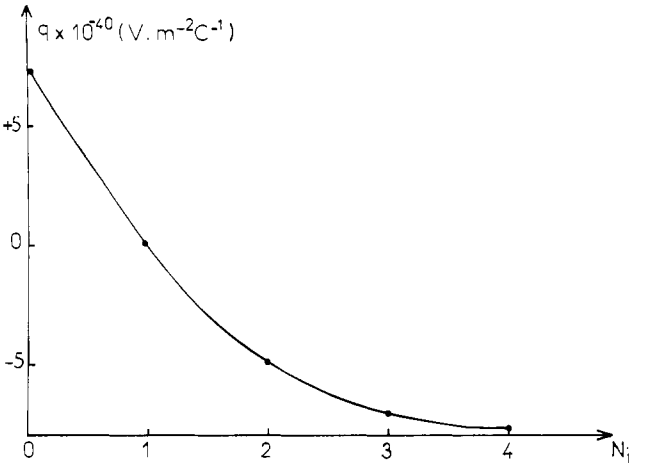

Figure 11. Variation of the electric field gradient q at the titanium nucleus with the occupational number Ni of the $e_2(d_{x^2-y^2}, d_{xy})$ metal orbitals.

Discussion

(1) Electric Field Gradient at the Titanium Nucleus. The experimental values of $A_\perp$ obtained here by ENDOR are much more accurate than those obtained by conventional ESR methods.[12] However, we shall not discuss these results since they do not alter the interpretation of the hf coupling made in the previous ESR study.

The quadrupolar parameter $P_\parallel$ is related to the nuclear spin I, to the quadrupolar moment Q, which measures the anisotropic distribution of charge within the nucleus, and to the electric field gradient (EFG) q at the nucleus, which measures the anisotropic distribution of charge surrounding that nucleus[15]

$$P_\parallel = \frac{3e^2Qq}{4I(2I-1)} \qquad (12)$$

The ratio $^{47}P_\parallel/^{49}P_\parallel = 2.55$ of the experimental values of $P_\parallel$ is in good agreement with the theoretical value 2.54 obtained by using the known values of the quadrupolar moments:[19] $^{47}Q = 0.29 \times 10^{-28}$ m^2 and $^{49}Q = 0.24 \times 10^{-28}$ m^2. The important chemical information obtained from $P_\parallel$ is the EFG, which is a direct measure of the electronic charge distribution around the nucleus. The experimental results give

$$q = -2.7 \times 10^{40} \text{ V m}^{-2} \text{ C}^{-1}$$

This EFG is essentially produced by the valence 3d electrons of the metal, with a small contribution of the ligand[20]

$$q = (1 - R_{3d})q_{val} + (1 - \gamma_\infty)q_{lig} \qquad (13)$$

where the quantities in parentheses represent respectively the Sternheimer shielding factor for the valence 3d electrons and the Sternheimer antishielding factor for the ligand electrons. These quantities describe the polarization of the core by the EFG of the 3d and ligand electrons.

Neglecting for the moment the ligand contribution, the EFG

(19) Hao, N.; Sayer, B. G.; Denes, G.; Bickley, D. G.; Detellier, C.; McGlinchey, M. J. *J. Magn. Reson.* **1982**, *50*, 50.
(20) White, L. K.; Belford, R. L. *J. Am. Chem. Soc.* **1976**, *98*, 4428.

created by the 3d electrons is expressed as[21]

$$(1 - R_{3d})q_{val} = (1 - R_{3d})(1/4\pi\epsilon_0)\sum_i N_i\langle 3\cos^2\theta_i - 1\rangle\langle r_i^{-3}\rangle \quad (14)$$

with $R_{3d} = 0.178$ and where N_i denotes the occupation number of the i^e 3d orbital. Values of $\langle r_i^{-3}\rangle$ depend on the effective charge on the metal and are found in the literature.[22] For an unpaired electron in the a_1 (d_{z^2}) orbital, the sign of q_{val}) will strongly depend on the occupation number of the $e_2(d_{x^2-y^2}, d_{xy})$ orbitals. Since the e^2(cot) orbital have the same energy as the 3d orbitals, the e_2 molecular bonding orbital is thus expected to have a significant metal character. However, the deep molecular e_1(Cp) orbital is of nearly purely ligand character.[9] The effect of occupation number of $d_{x^2-y^2}$, d_{xy} orbitals on the EFG is shown in Figure 11. The EFG is found to vary between $+7.2 \times 10^{40}$ V m^{-2} C^{-1} for a $d^1(Ti^{3+})$ configuration and -7.7×10^{40} V m^{-2} C^{-1} for a $d^5(Ti^-)$ configuration. Our experimental value -2.7×10^{40} V m^{-2} C^{-1} points to a significant occupation of the $d_{x^2-y^2}$ and d_{xy} orbitals: $N_{x^2-y^2} + N_{xy} \simeq 1.5$. This result agrees with the low effective charge on the metal, between 0 and +1, found by UPS[11] and by the effective spin orbit coupling constant λ.[12] It should be emphasized that a small occupation of d_{xz} and d_{yz} orbitals, which have a positive contribution to the EFG, will increase its value, while a small occupation of the 4s orbital will have no contribution to it.

To calculate correctly the EFG, it should be necessary to perform a Mulliken population analysis of the molecular orbital coefficients, which to our knowledge is not available for CpTicot. It seems reasonable to neglect the ligand contribution to the EFG if we express it by the point charge approximation[21]

$$(1 - \gamma_\infty)q_{lig} = (1 - \gamma_\infty)(1/4\pi\epsilon_0)\sum_L Z_L(3\cos^2\theta_L - 1)R_L^{-3} \quad (15)$$

Owing to the large Ti–C and Ti–H distances and to the small effective charges Z_L on carbon and proton atoms, this contribution should be small, even if γ_∞ is large and not known with precision ($\gamma_\infty \sim -10$ to -30).[21] For example, by using θ_L and R_L from crystallographic data[8] and Z_L from a INDO SCF molecular orbital calculation,[9] one obtains

$$(1 - \gamma_\infty)q_{lig} \simeq (0.1\text{–}0.2) \times 10^{40} \text{ V m}^{-2} \text{ C}^{-1}$$

(2) Proton Hyperfine Interaction. The important chemical information obtained from the titanium–proton hf coupling is the metal–proton distance R_N. Since R_N is higher than 2 Å, the simple point dipole–dipole approach can be used to interpret the dipolar hf interaction. In this simple level of approximation the dipolar coupling is expressed as

$$A^{dip} = \frac{g\beta g_N\beta_N}{R_N^3}[3\cos^2(\theta_N - \theta) - 1] \quad (16)$$

Assuming a spin density $\rho_M = 1$ on the metal atom and using the experimental values of A_i^{dip}, the mean values of R_N are 3.2 (5) and 3.1 (1) Å for cot and Cp rings, respectively. These distances are close to the values 3.19 and 3.00 Å deduced from analysis of X-ray data[8,13] (Table IV); however, it is not sure that the small discrepancies of 0.06 and 0.11 Å are only due to experimental uncertainties. Other sources of discrepancies could be (i) differences of about 0.1 Å in the distances due to the fact that X-ray data were obtained from a CpTicot single crystal at room temperature and that ENDOR measurements were performed on isolated molecules in a toluene matrix at low temperature and (ii) a contribution to the dipolar coupling coming from a finite spin density $\rho_\pi \ll 1$ in carbon $P_\pi(2p_z)$ orbitals. It follows that the resulting hf interaction should be slightly orthorhombic, although the simple point dipole–dipole expression 16 implies an axial dipolar tensor

$$A_1^{dip} = A_2^{dip} = -A_3^{dip}/2 \quad (17)$$

There is experimental evidence (cf. Table II) that the dipolar tensor for cot rings is orthorhombic, and thus it appears likely that the effect of spin density on carbon atoms of cot rings could contribute to the observed discrepancy between X-ray and ENDOR data.

From the isotropic hf interaction A_{iso} we obtain spin densities on protons ρ_H(cot) = $+6.2 \times 10^{-3}$ and ρ_H(Cp) = $+2.9 \times 10^{-3}$. They arise from the direct delocalization of the unpaired electron on the s hydrogen orbital. By comparison INDO SFC molecular orbital calculations[8] gave ρ_H(cot) = $+1 \times 10^{-3}$ and ρ_H(Cp) = $+2.5 \times 10^{-3}$. Although the agreement is fair for Cp rings, there is a significant discrepancy for cot rings, which could partly arise from the contribution of a spin-polarization of the C–H bond due to a negative spin density ρ_π in carbon P_π orbitals.

Comparison in I and II of the temperature dependence of the ^{1}H ENDOR line shapes gives some information concerning the dynamics of ring reorientation. It is noteworthy that the presence of a methyl group on the Cp ring completely hinders the reorientation of this ring but does not affect the reorientation of the cot ring, which is observed above 60 K for both I and II compounds.

This strongly suggests that intramolecular potentials have negligible contribution to the ring dynamics. Similar conclusions were obtained from ENDOR studies of dibenzene vanadium in single crystal host lattice or in frozen toluene solutions. Furthermore, the ENDOR spectra at temperatures between 60 and 90 K are always the superposition of a powderlike and single crystallike spectra, showing that in this temperature range there is always coexistence of molecules with fast reorienting rings and molecules with "static" rings. This points to the existence of a range of activation energies rather than a well-defined one controlling the ring motion. In the latter case we would expect a gradual modification of the line shape due to the increase of the reorientation frequency.[2] The existence of a range of activation energies can be related to a random character of the orientation of toluene molecules constituting the solvent cages. The evolution with temperature of the matrix ENDOR line shape shows that the motion of cage molecules appears at the same temperature as the ring reorientation of the sandwich complex. It is possible that the onset of motion of toluene molecules adjacent to the complex progressively weakens the CpTicot–toluene molecular interaction and thus decreases the activation energy for the ring reorientation.

Conclusion

In this work we have measured the hyperfine interaction parameters of the title compounds, without having recourse to single crystal dilution in a diamagnetic matrix. We have also detected, in dilute frozen solutions, ^{47}Ti and ^{49}Ti nuclei with natural isotope abundance and measured their hf parameters and in particular the quadrupole interaction with precision.

Furthermore, in solid solution, we show that the molecular motion has a distinct effect on the line shape. The rapid ring rotation around the metal-to-ring axis exhibits single crystallike spectra whereas a slowed down rotation gives a powder spectrum.

It is believed that similar studies can be extended to paramagnetic organometallic compounds and especially those of zirconium which are being progressively discovered and for which ESR data are rather scanty.

Acknowledgment. The technical assistance of D. Simons and J. Henique is gratefully acknowledged.

(21) Kita, S.; Hashimoto, M.; Iwaizumi, M. *J. Magn. Reson.* **1982**, *46*, 361.
(22) Clementi, E. *Phys. Rev.* **1964**, *135*, 980. Clementi, E. *J. Chem. Phys.* **1964**, *41*, 295; **1964**, *41* (part 2 suppl).
(23) Fantucci, P.; Balzarini, P.; Valenti, V. *Inorg. Chim. Acta* **1977**, *25*, 113.
(24) McConnell, H. M.; Strathdee, J. *Mol. Phys.* **1959**, *2*, 129.
(25) Kivelson, D.; Lee, S. K. *J. Chem. Phys.* **1964**, *41*, 1896.